TRACE AND YOHKOH OBSERVATIONS OF HIGH-TEMPERATURE PLASMA IN A TWO-RIBBON LIMB FLARE

H. P. Warren[1], J. A. Bookbinder[1], T. G. Forbes[2], L. Golub[1], H. S. Hudson[3], K. Reeves[1], and A. Warshall[1]

ABSTRACT

The ability of the Transition Region and Coronal Explorer (TRACE) to image solar plasma over a wide range of temperatures ($T_e \sim 10^4$–10^7 K) at high spatial resolution ($0\rlap{.}''5$ pixels) make it a unique instrument for observing solar flares. We present TRACE and Yohkoh observations of an M2.4 two-ribbon flare that began on 1999 July 25 at about 13:08 UT. We observe impulsive footpoint brightenings that are followed by the formation of high-temperature plasma ($T_e \gtrsim 10$ MK) in the corona. After an interval of about 1300 s cooler loops ($T_e < 2$ MK) form below the hot plasma. Thus the evolution of the event supports the qualitative aspects of the standard reconnection model of solar flares. The TRACE and Yohkoh data show that the bulk of the flare emission is at or below 10 MK. The TRACE data are also consistent with the Yohkoh observations of hotter plasma ($T_e \sim 15 - 20$ MK) existing at the top of the arcade. The cooling time inferred from these observations is consistent with a hybrid cooling time based on thermal conduction and radiative cooling.

Subject headings: Sun: activity — Sun: corona — Sun: flare

1. INTRODUCTION

Understanding how energy is released in solar flares is a central question in astrophysics. TRACE, which is a high-resolution imaging telescope launched last year as part of NASA's Small Explorer program, has several capabilities that make it a unique instrument for flare observations. TRACE can image plasma over a very wide range of plasma temperatures (10^4–10^7 K). The sensitivity of TRACE to high temperature plasma is derived from the presence of the Ca XVII 193 Å and Fe XXIV 192 Å flare lines in its 195 Å channel in addition to Fe XII. Thus TRACE can observe the pre-flare corona, the response of the chromosphere to energy deposition, the formation of high temperature flare loops in the corona, and the cooling of post-flare loop arcades. TRACE also has a spatial resolution of $1''$ ($0\rlap{.}''5$ pixels). This is higher than the nominal resolution of $2''$ to $5''$ achieved with previous instruments used to observe flares (Vaiana et al. 1977; Underwood et al. 1976; Tousey et al. 1977; Tsuneta et al. 1991).

One difficulty with TRACE flare observations is the non-uniqueness of the temperatures derived from the filter ratios. Abundance variations further complicate the interpretation of the TRACE filter ratios since the signal in the 195 Å channel at flare temperatures is dominated by line emission from low first ionization potential (FIP) ions while the other EUV channels contain continuum (mainly H, which is high FIP) emission (Feldman et al. 1999). This continuum flare emission is also generally weak, making reliable filter ratios difficult to determine for many flare observations. Thus observations of flares with both TRACE and Yohkoh are essential for deriving a complete observational picture of solar flares.

In this paper we present TRACE and Yohkoh observations of an M2.4 limb flare that began in NOAA active region 8639 on 1999 July 25 at about 13:08 UT. This event is one of the few large flares co-observed by both TRACE and Yohkoh to date. A dramatic coronal mass ejection associated with the event was detected by the LASCO coronagraph on SoHO.

2. INSTRUMENTATION

TRACE is based on a 30 cm Cassegrain telescope. The primary and secondary mirrors are divided into quadrants and a rotating shutter is used to select which quadrant is illuminated. Three of the quadrants are coated with multilayers for imaging at EUV wavelengths. The multilayer coatings have peak sensitivities at approximately 173, 195, and 284 Å. The fourth quadrant is coated with aluminum and magnesium fluoride for imaging very broad wavelength ranges near 1216, 1550, 1600, and 1700 Å. Images in all of the wavelengths are projected onto a single detector, a 1024×1024 CCD. Each CCD pixel represents a solar area about $0\rlap{.}''5$ on a side. The instrument is described in detail by Handy et al. (1999). The initial in-flight performance is reviewed by Golub et al. (1999) and Schrijver et al. (1999).

For this event 171, 195, and 1216 Å images were taken at a cadence of about 60 s, while 1550, 1600, and 1700 Å images were taken at a cadence of about 900 s. Unfortunately, due to an error in the observing sequence, high-resolution EUV images were not taken and only low resolution ($4''$ pixels) TRACE 171 Å and 195 Å images are available for this event.

The Soft X-Ray Telescope (SXT) on Yohkoh (Tsuneta et al. 1991) is a grazing incidence telescope with a nominal spatial resolution of about $5''$ ($2\rlap{.}''46$ pixels). Temperature discrimination is achieved through the use of several focal

[1] Harvard-Smithsonian Center for Astrophysics, 60 Garden Street MS 58, Cambridge, MA 02138, hwarren@cfa.harvard.edu

[2] Institute for the Study of Earth, Ocean, and Space (EOS), University of New Hampshire, Durham, NH 03824

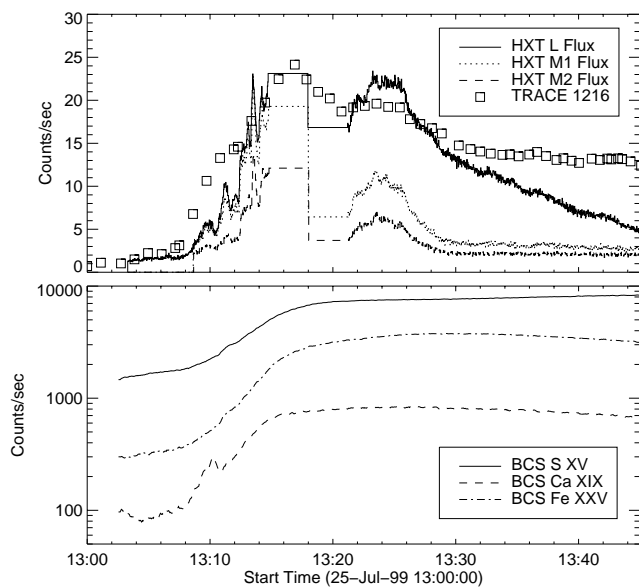[3] Solar Physics Research Corp., 4720 Calle Desecada, Tucson, AZ 85718

Fig. 1.— (top panel) Light curves from the HXT L, M1, M2 channels, and the flare footpoints seen in the TRACE 1216 Å images. The TRACE 1216 Å light curve has been scaled to have the same range as the HXT L light curve. (bottom panel) BCS Fe XXIV, Ca XIX, and S XV light curves. The total counts in each channel are plotted. The flat maxima in the BCS channels reflect detector saturation.

plane filters. The Bragg Crystal Spectrometer (BCS) on Yohkoh (Culhane et al. 1991) provides uncollimated observations of the Sun in four narrow wavelength ranges near the resonance lines of Fe XXVI, Fe XXV, Ca XIX, and S XV with a temporal resolution as high as 3 s. We also consider observations of this flare taken with the Yohkoh Hard X-Ray Telescope (HXT) (Kosugi et al. 1991). HXT uses a Fourier-synthesis technique to take images in four hard x-ray (HXR) energy bands with a collimator response (FWHM) of about $8''$.

Yohkoh entered flare mode for this event at about 13:08 UT. The flare response provided full-resolution SXT images of a region $2'\!.6$ square at a cadence of about 2 s. High cadence BCS and HXT data were also taken. There is a short gap in the Yohkoh SXT and HXT data from 13:14 to 13:21 UT due to a data downlink. All of the Yohkoh and TRACE data were processed using the standard IDL SolarSoft routines (Freeland & Handy 1998).

3. OBSERVATIONS

Early in the event two narrow brightenings, or ribbons, become evident in the TRACE 1216 Å images. As shown in Figure 1, the evolution of the footpoints is temporally correlated with the HXR emission observed by HXT during the impulsive phase of the flare. In contrast to the HXR emission, however, the emission from the flare footpoints evident in the TRACE 1216 Å images does not decay rapidly. This suggests different mechanisms are responsible for the TRACE UV footpoint emission at different times.

Several TRACE and Yohkoh images from this event are

shown in Figure 2. An obvious feature of the TRACE images is the bright emission in the 195 Å channel that has no strong counterpart in the 171 Å channel. This behavior is consistent with the spectrally and spatially resolved Skylab SO82A Spectroheliograph flare observations (e.g., Cheng & Widing 1975) which showed that near the peak of a flare the high temperature line emission ($T_e > 10$ MK) dominated lower temperature line emission ($T_e < 3$ MK) within the flare loops. As the images in Figure 2 indicate, the bright emission seen in the TRACE 195 Å images is also well correlated spatially with the emission seen in the SXT images.

This high temperature flare plasma is also evident in the TRACE 171 Å images from the continuum emission in that passband. This emission is weak compared to the surrounding active region, however, and it is difficult to make quantitive measurements of electron temperatures from these TRACE data. More reliable measurements of electron temperature can be derived from the Yohkoh filter ratios. As illustrated by Figure 3, the bulk of the flare emission is characterized by electron temperatures of $\lesssim$ 10 MK and volume emission measures of $\lesssim 2 \times 10^{47}$ cm^{-3}. We have used parameters derived from the SXT images to compute synthetic spectra, which we convolved with the TRACE instrument response functions. The spatial and temporal variations are reproduced very well, although the count rates predicted for TRACE are systematically higher than what is observed by about a factor of 3. There are a number of possible explanations for this, such as errors in the instrumental calibrations, which we are currently investigating. The consistency of the TRACE and Yohkoh emission shows that the bulk of the flare emission measure is at or below 10 MK.

Evident in Figure 3 is a hotter component of flare plasma at the top of the arcade with temperatures of 15-20 MK. Such a component has been observed in a number of other SXT flares (e.g., Tsuneta et al. 1997; Nitta & Yaji 1997). Since Fe XXIV, which has a temperature of formation of about 20 MK (Arnaud & Raymond 1992), is the dominant contributor to emission in the TRACE 195 Å channel during the peak of a large flare, one would expect this bandpass to be particularly sensitive to this hotter component. The TRACE 195 Å images, however, are generally similar to the SXT images and show no excess brightness near the very top of the arcade. As shown in Figure 4 the physical parameters derived from SXT accurately predict the TRACE count rates in this hotter region relative to bulk of the flare plasma. Thus we conclude that the TRACE observations are consistent with the 15-20 MK component seen in SXT. The TRACE 195 Å images are not bright in this region since the rapid decline of the emission measure above the arcade more than counterbalances the increased emissivity of Fe XXIV at the higher temperature.

It is not until well into the event (about 13:31:42 UT) that bright loops appear in both the TRACE 171 Å 195 Å images. The TRACE filter ratios and the absence of cor-
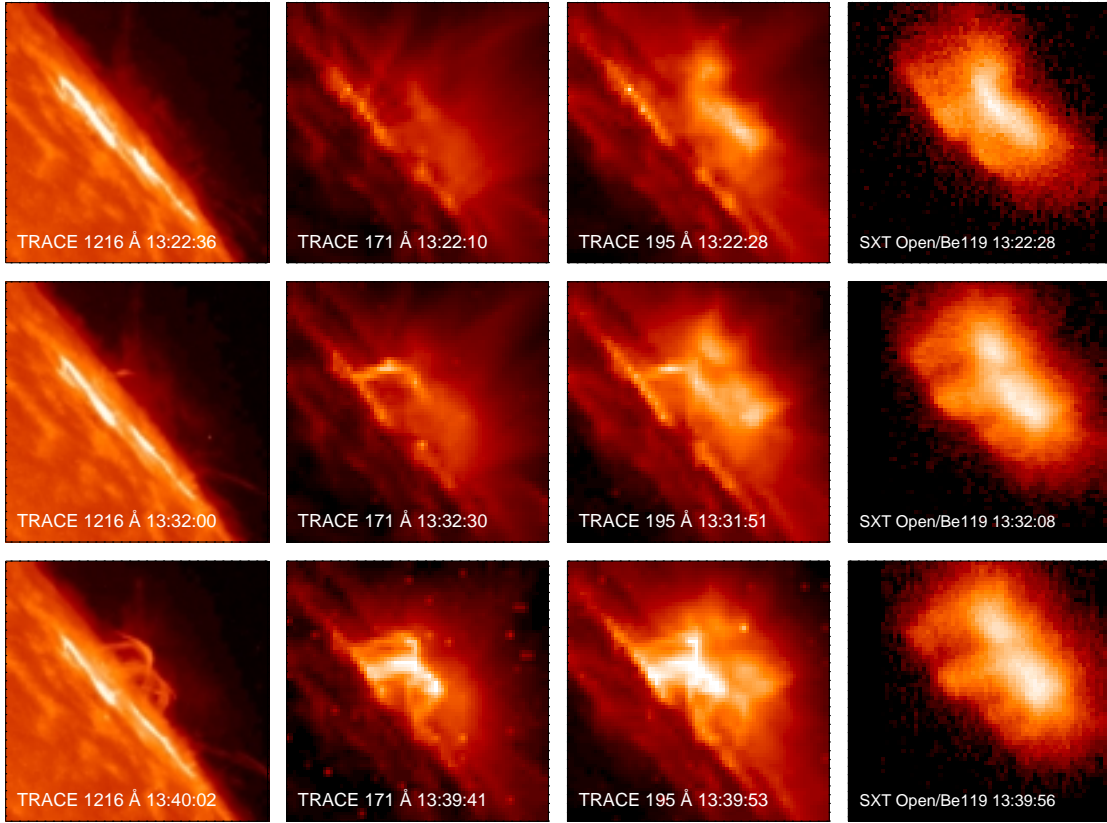
Fig. 2.— TRACE 1216, 171, and 195 Å images and SXT Be 119 μm filter images from the 1999 July 25 M2.4 flare. The TRACE and SXT images have been co-aligned empirically. The TRACE EUV images are low resolution ($4''$ pixels) and have been interpolated. The TRACE 1216 Å images are full resolution.

responding emission in the SXT images indicate temperatures of < 2 MK for these loops. Surprisingly, the first bright loops evident in the TRACE 1216 Å images occur at 13:32:00 UT, almost simultaneously with the appearance of the < 2 MK loops. Since significant high-temperature emission does not appear until about 13:10 UT (see Figure 1), the upper bound on the cooling time is about 1300 s.

The problem of how high-temperature flare plasma cools has been considered by Cargill et al. (1995). They derive a simple formula for the cooling time which is a hybrid of the linear radiative cooling time ($t_r = 3.47 \times 10^3 n_e^{-1} T_e^{3/2}$ in cgs units) and the linear conductive cooling time ($t_c = 4 \times 10^{-10} n_e L^2 T_e^{-5/2}$). The parameters n_e, T_e, and L are the electron density, electron temperature, and loop half-length at the beginning of the cooling phase.

We have used physical quantities derived from the observations to estimate the cooling times. A loop half-length of 5×10^9 cm was estimated by tracing out the first post-flare loop evident in TRACE. Since we do not account for projection effects, this estimate is a lower bound on the true loop length and thus on t_c. The electron temperatures and emission measures derived from SXT filter ratios taken during the early phase of the flare (13:09 UT) are approximately 1.0×10^7 K and 5×10^{45} cm^{-3}. The density is related to the line of sight emission measure by

$n_e = (EM/df)^{1/2}$, where d is the path length and f is the filling factor. The TRACE 1216 Å images of post-flare loops for this event suggest that the flare loops are very fine and not well resolved by SXT. If we assume, based on the fine structure evident in the TRACE 1216 Å images for this event, that this emission is confined to a size of $\lesssim 1''$, we obtain a density of $\gtrsim 5 \times 10^{10}$ cm^{-3}. These parameters yield a radiative cooling time of $\lesssim 2.2 \times 10^3$ s and a conductive cooling time of $\gtrsim 1.6 \times 10^3$ s. The hybrid cooling time is 1.4×10^3 s, which is close to what is observed.

4.   DISCUSSION

We have presented TRACE and Yohkoh observations of a two-ribbon flare. We observe impulsive footpoint brightenings that are quickly followed by the formation of high-temperature loops in the corona. After an interval of about 1300 s cooler loops form below the hot loops. Thus these observations support the qualitative aspects of the standard model of flares based on reconnection (e.g., Forbes & Acton 1996). The TRACE and Yohkoh data show that the bulk of the flare emission is at or below 10 MK. Both the TRACE and Yohkoh observations are also consistent with a hotter ($T_e \sim 15 - 20$ MK) plasma existing at the top of the arcade. The cooling of the flare plasma in this event is roughly consistent with the hybrid cooling time of
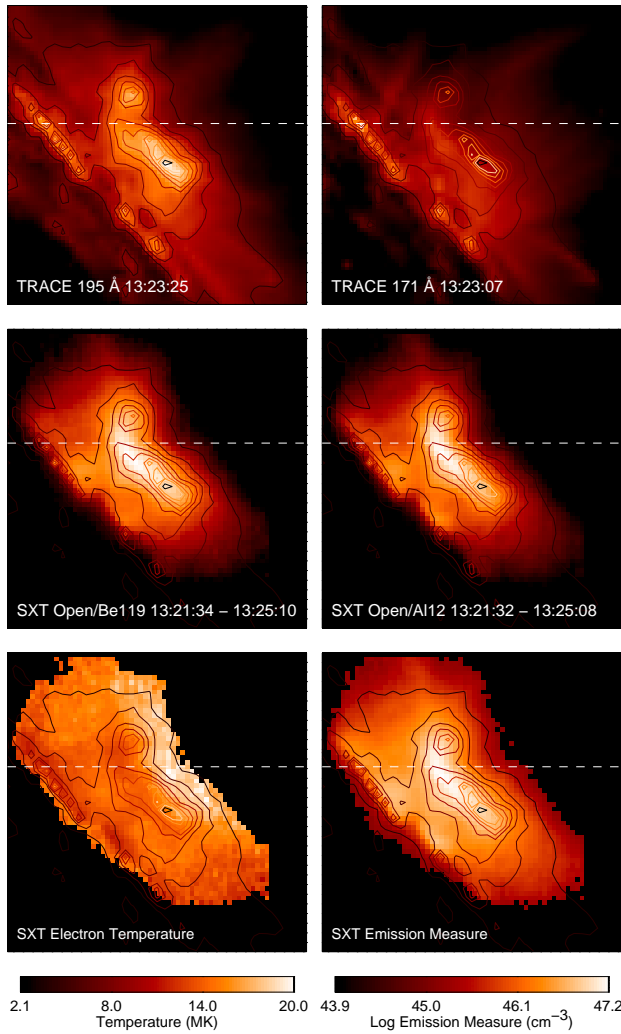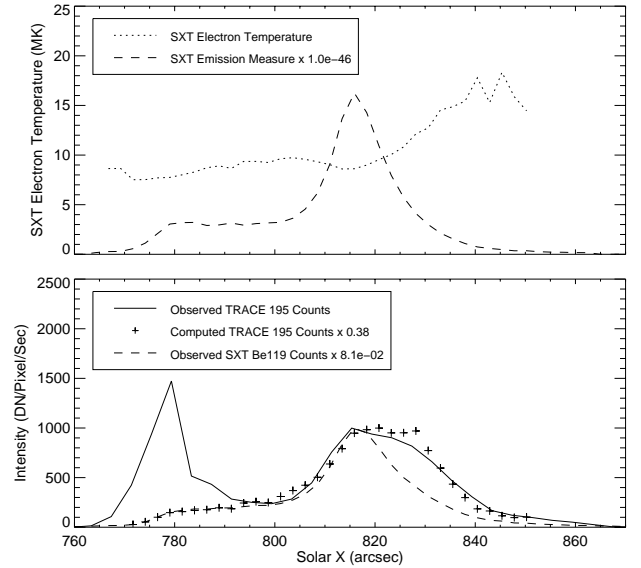
Fig. 4.— The observed TRACE count rates in the 195 Å channel as a function of position for the region indicated in Figure 3. Note the clear separation of the cool Fe XII footpoint response (left) and the hot Fe XXIV response of the coronal loops (right). A constant background level for the TRACE intensities was estimated from the TRACE emission at the largest heights.

Fig. 3.— (top panel) TRACE 171 Å and 195 Å images. (middle panel) SXT Be 119 μm and Al 11.6 μm images. These images have been constructed by summing over all of the images with the same filter during the interval indicated. (bottom panel) Electron temperatures and emission measures derived from the SXT filter ratios. The countours in all of the panels are dervied from the TRACE 195 Å image. Data from the region indicated by the dashed line are plotted in Figure 4.

Cargill et al. (1995).

The full-resolution TRACE 1216 Å images suggest relatively small filling factors for flare loops relative to SXT pixels. Inspection of some full-resolution TRACE 195 Å flare observations also suggest very small filling factors, since it is difficult to find isolated high temperature loops in these images. In contrast, the lower temperature post-flare plasma always appears as loops. This difference in morphology is evident even in the low-resolution TRACE EUV images shown in Figure 2. The low temperature (< 2 MK) plasma seen in the post-flare phase of the event appears loop-like, while the high temperature (> 10 MK) plasma does not. The morphology of high temperature flare plasma is of considerable interest and will be pursued in a future publication.

REFERENCES

Arnaud, M., & Raymond, J. 1992, ApJ, 398, 394

Cargill, P. J., Mariska, J. T., & Antiochos, S. K. 1995, ApJ, 439, 1034

Cheng, C.-C., & Widing, K. G. 1975, ApJ, 201, 735

Culhane, J. L., et al. 1991, Sol. Phys., 136, 89

Feldman, U., Laming, J. M., Doschek, G. A., Warren, H. P., & Golub, L. 1999, ApJ, 511, L61

Forbes, T. G., & Acton, L. W. 1996, ApJ, 459, 330

Freeland, S. L., & Handy, B. N. 1998, Sol. Phys., 182, 497

Golub, L., et al. 1999, Phys. Plasmas, 6, 2205

Handy, B. N., et al. 1999, Sol. Phys., in press

Kosugi, T., et al. 1991, Sol. Phys., 136, 17

Nitta, N., & Yaji, K. 1997, ApJ, 484, 927

Schrijver, C. J., et al. 1999, Sol. Phys., in press

Tousey, R., Bartoe, J. D. F., Brueckner, G. E., & Purcell, J. D. 1977, Appl. Opt., 16, 870

Tsuneta, S., et al. 1991, Solar Phys., 136, 37

Tsuneta, S., Masuda, S., Kosugi, T., & Sato, J. 1997, ApJ, 478, 787

Underwood, J. H., Milligan, J. E., Deloach, A. C., & Hoover, R. B. 1976, Appl. Opt., 16, 858

Vaiana, G. S., Van Speybroeck, L., Zombeck, M. V., Krieger, A. S., Silk, J. K., & Timothy, A. 1977, Space Science Instrumentation, 3, 19